Supplementary Information

Specific Visual-volumetric Sensor for Mercury Ion Based on Smart Hydrogel

Shenghai Zhang,* Wenzhong Qu, Simeng Chen, Dian Guo, Kaixi Xue, Run Li, Jidong Zhang, and Lingjian Yang

School of Chemistry and Chemical Engineering, Ankang Univerisity, Quality Supervision and Inspection Centre of Se-enriched Food of Shaanxi Province, Shaanxi University Innovation Research Institute of Advanced Energy Storage Materials and Battery Technology for Future Industrialization, Ankang Research Centre of New Nano-materials Science and Technology Research Centre, Ankang, Shaanxi province, 725000, P. R. China

* Corresponding Author: E-mail: zhshhai512@163.com; fax: +86 0915 3261415

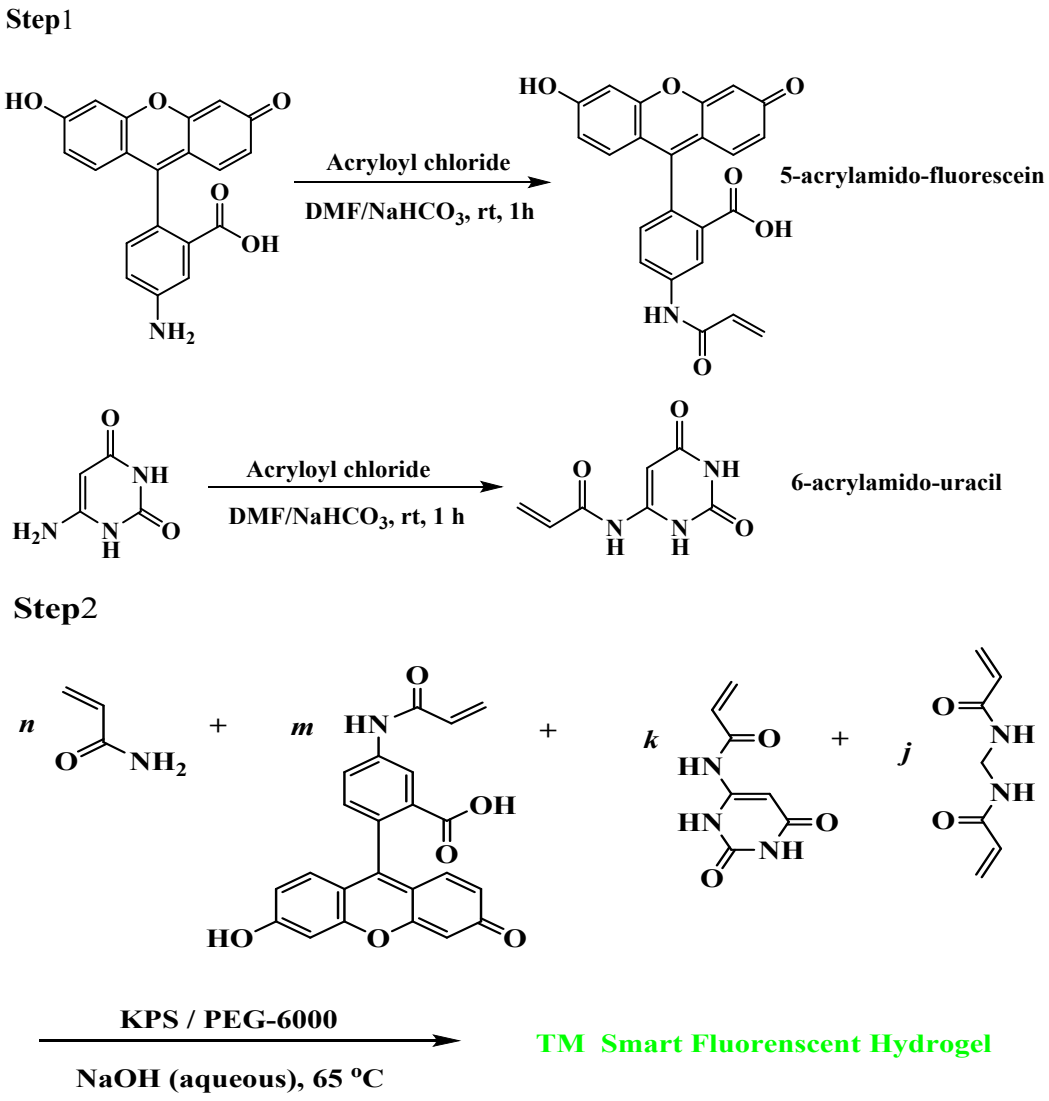

Fig. S1 Synthetic route of the smart fluorescent hydrogel

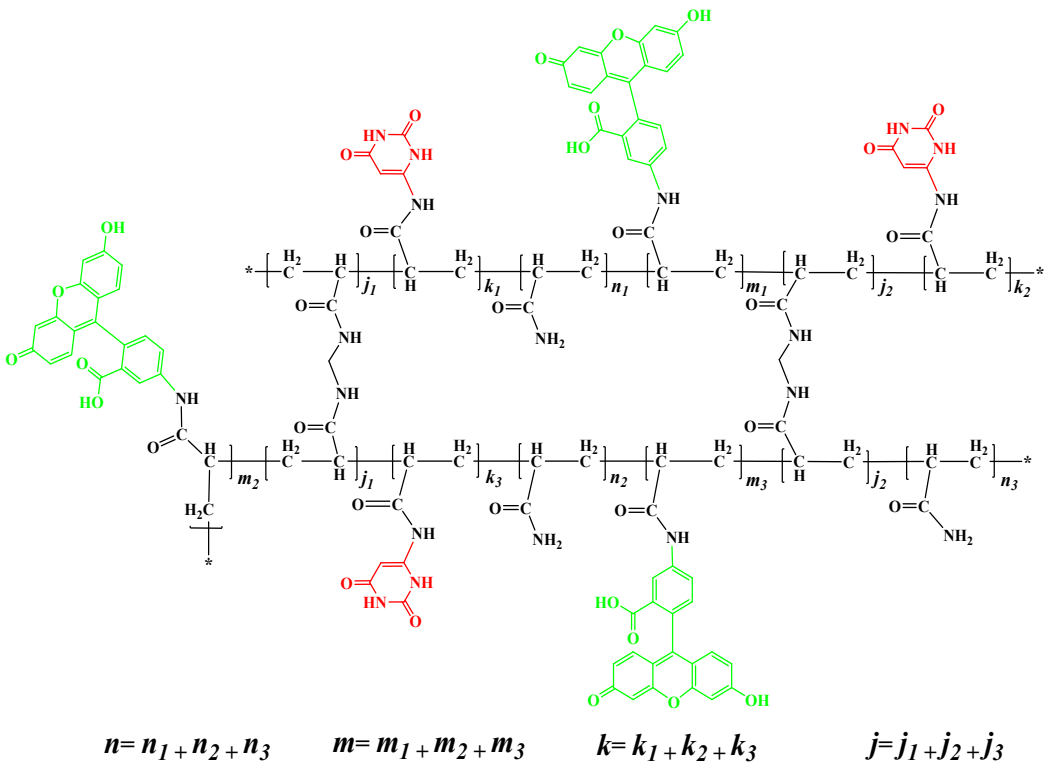

Fig. S2 The structure of the smart fluorescent hydrogel

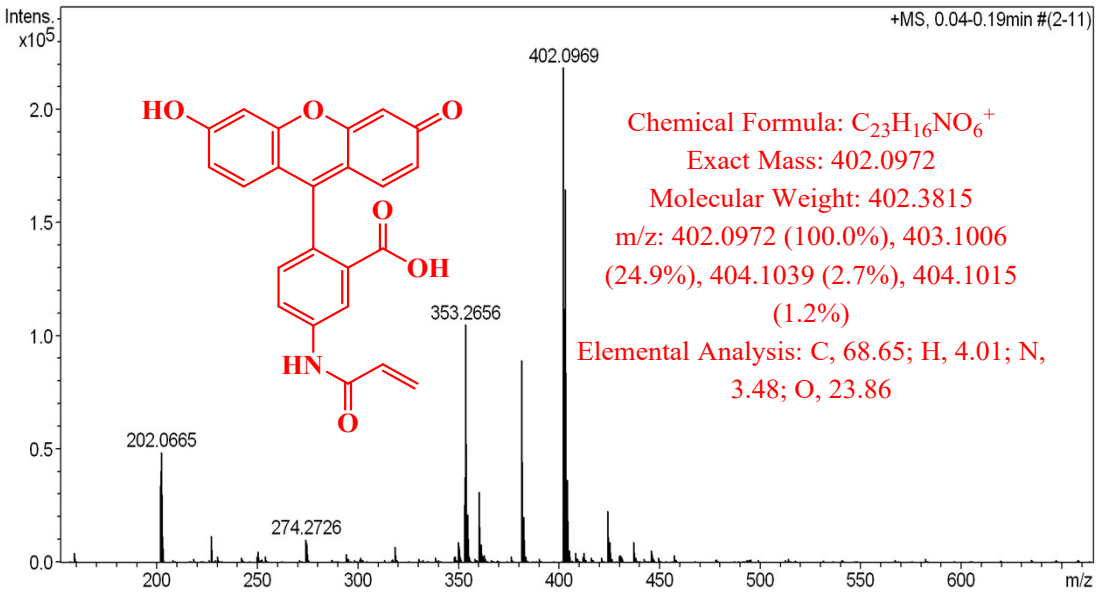

Fig. S3 Mass spectrum of the prepared 5-acrylamido-fluorescein

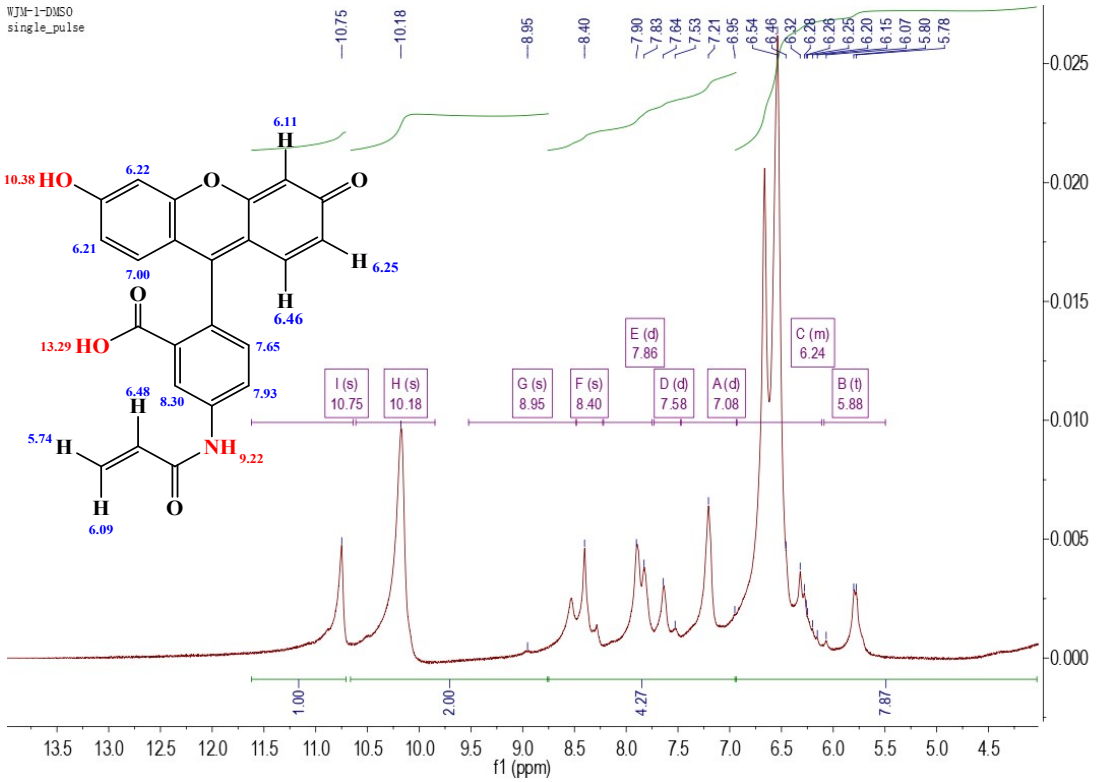

Fig. S4 ^{1}H NMR spectrum of 5-acrylamido-fluorescein

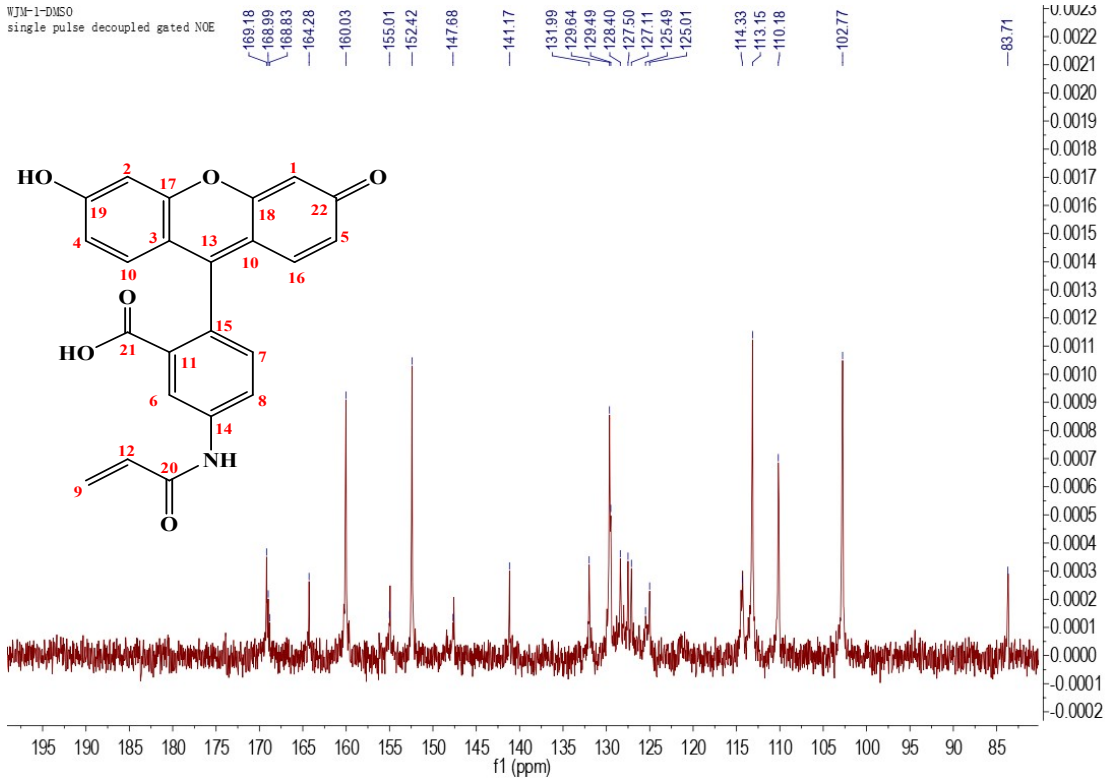

Fig. S5 ^{13}C NMR spectrum of 5-acrylamido-fluorescein

Fig. S6 Response characteristics of fluorescent hydrogels to Hg^{2+}. Volume changes of the fully swelled fluorescent hydrogel after soaking in $3.0 \times 10^{-4}\ mol \cdot L^{-1}$ NaCl solution (left) and $1.0 \times 10^{-4}\ mol \cdot L^{-1}$ $Hg(NO_3)_2$ solution (right) for 30 min.

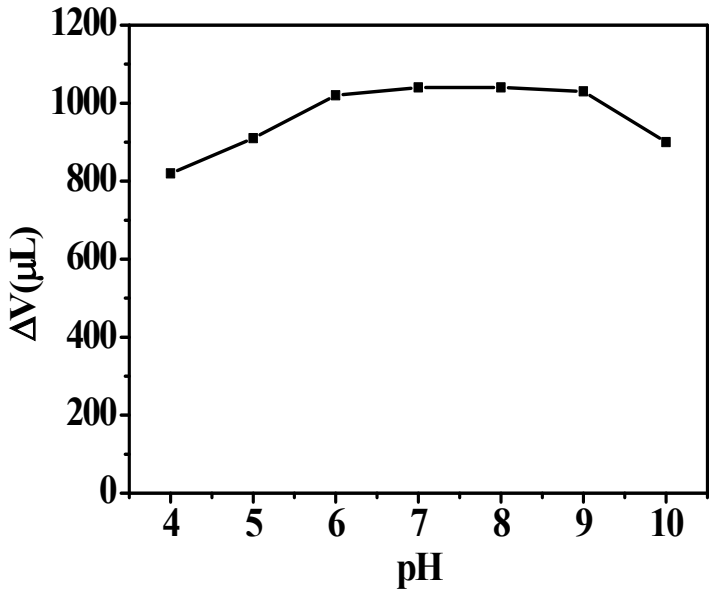

Fig. S7 Effect of pH on the Hg^{2+}-induced volume shrinkage of the obtained hydrogel. Hg^{2+}, 5.0×10^{-5} $mol \cdot L^{-1}$; pH 4~10, by adding 0.2 M NaOH to B-R buffer (0.04 M H_3PO_4, HAc and H_3BO_3).

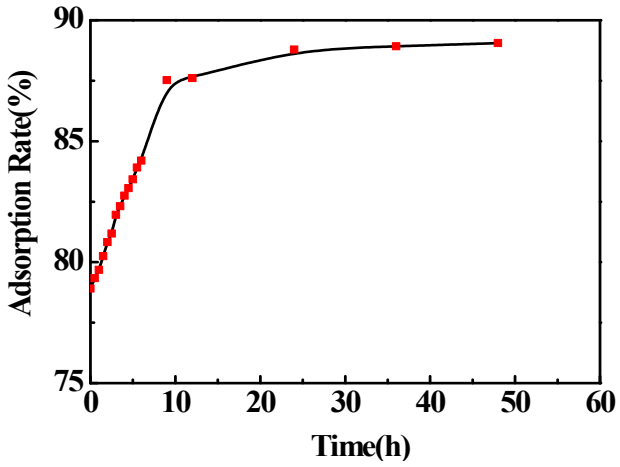

Fig. S8 Effect of time on the adsorption rate for Hg^{2+}

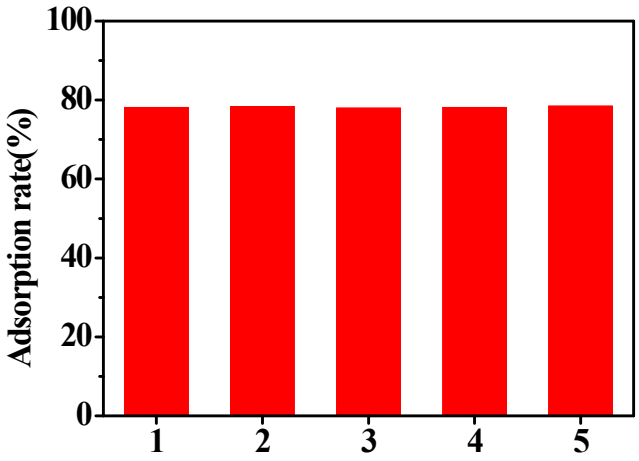

Fig. S9 The adsorption rate of 30 minutes for Hg^{2+}

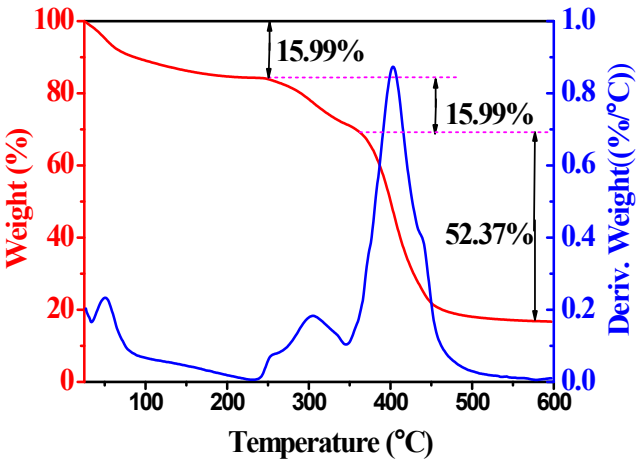

Fig. S10 TGA result of the obtained hydrogel. Rate of the temperature rise, 5.0 ℃/min; Temperature range, 27~600 ℃.

Table S1 Comparison of the reported and the present nitrogen base-based sensors for Hg^{2+} determination

Sensor type	Advantages	Disadvantages	Ref.
Electrochemical sensor	High sensitivity, fast response, and can be used in opaque system	Complicated in sensor preparation, determination results affected by non-specific adsorption, and electrochemistry workstation is required	[1-20]
Colorimetric sensor	Low-cost, naked-eye readout or a simple instrument is require-ment, and can be used for field detection	Color vision difference limits the sensitivity, which usually makes it is difficult to accurately quantify and generally be used for qualitative or semi-quantitative analysis	[21-33]
Fluorescence sensor	High sensitivity, fast response speed, wide linear range and short time consuming	Environmental factors greatly influenced the determination results, and there may exist the problems such as photobleaching and low fluorescent intensity, etc; Fluorescence spectrophotometer is required and rarely available for field detection	[34-56]
The present sensor	Easy operate, ultra - low cost and suitable for on-site inspection; Naked-eye signal readout in line with human's perception nature of "seeing is believing" and power-free of instrument requirement	Sensitivity needs to be further improved that limited by the currently obtained sensing materials	—

References

[1] X. H. Niu, Y. L. Ding, C. Chen, H. L. Zhao, M. B. Lan. *Sensor. Actuat. B-Chem.*, 2011, **158**, 383.

[2] Y. Lai, Y. Ma, L. Sun, J. Jia, J. Weng, N. Hu, W. Yang, Q. Zhang. *Electrochim. Acta*., 2011, **56**, 3153.

[3] H. Park, S. Hwang, K. Kim. *Electrochem. Commun.*, 2012, **24**, 100.

[4] M. Ebrahimi, J. Raoof, R. Ojani, Z. Bagheryan. *Anal. Biochem.*, 2015, **488**, 12.

[5] E. Xiong, L. Wu, J. Zhou, P. Yu, X. Zhang, J. Chen. *Anal. Chim. Acta*, 2015, **853**, 242.

[6] C. Tortolini, P. Bollella, M. Antonelli, R. Antiochia, F. Mazzei, G. Favero. *Biosens. Bioelectron.*, 2015, **67**, 524.

[7] J. Jing, G. Hong, F. Ji, L. Jing, Q. Hong, B. Nian. *Anal. Chim. Acta*, 2016, **908**, 95.

[8] J. Li, L. Lu, T. Kang, S. Cheng. *Biosens. Bioelectron.*, 2016, **77**, 740.

[9] G. Zeng, C. Zhang, D. Huang, C. Lai, L. Tang, Y. Zhou, P. Xu, H. Wang, L. Qin, M. Cheng. *Biosens. Bioelectron*., 2016, **90**, 542.

[10] Z. Zhang, X. Fu, K. Li, R. Liu, D. Peng, L. He, M. Wang, H. Zhang, L. Zhou. *Sensor. Actuat. B-Chem*., 2016, **225**, 453.

[11] C. Mei, D. Lin, C. Fan, A. Liu, S. Wang, J. Wang. *Biosens. Bioelectron.*, 2016, **80**, 105.

[12] M. Hong, M. Wang, J. Wang, X. Xu, Z. Lin. *Biosens. Bioelectron*., 2017, **94**, 19.

[13] Y. Zhang, G. Chu, Y. Guo, W. Zhao, Q. Yang, X. Sun. *J. Electroanal. Chem*., 2018, **824**, 201.

[14] S. Cao, H. Hu, R. Liang, J. Qiu. *J. Electroanal. Chem.*, 2020, **856**, 113494.

[15] L. He, L. Cheng, Y. Lin, H. Cui, N. Hong, H. Peng, D. Kong, C. Chen, J. Zhang, G. Wei, H. Fan. *J. Electroanal. Chem*., 2018, **814**, 161.

[16] S. Wu, B. Zhang, F. Wang, Z. Mi, J. Sun. *Biosens. Bioelectron*., 2018, **104**, 145.

[17] L. Zhao, Y. Wang, G. Zhao, N. Zhang, Y. Zhang, X. Luo, B. Du, Q. Wei. *J. Electroanal. Chem.,* 2019, **848**, 113308.

[18] Y. Yu, Y. Chao, R. Gao, J. Chen, H. Zhong, Y. Wen, X. Ji, J. Wu, J. He. *Biosens. Bioelectron.*, 2019, **131**, 207.

[19] X. Wang, C. Xu, Y. Wang, W. Li, Z. Chen. *Sensor. Actuat. B-Chem*., 2021, **343**, 130151.

[20] Y. Shao, Y. Dong, L. Fan, W. Xu, L. Bin, L. Wang, D. Li, S. Zhao. *Microchem. J*., 2022, **177**, 107290.

[21] T. Li, S. Dong, E. Wang. *Anal. Chem.*, 2009, **81**, 2144.

[22] C. J. Yu, T. L. Cheng, W. L. Tseng. *Biosens. Bioelectron*., 2009, **25**, 204.

[23] S. M. Jia, X. F. Liu, P. Li, D. M. Kong, H. X. Shen. *Biosens. Bioelectron*., 2011, **27**, 148.

[24] Y. Y. Zhu, Y. L. Cai, Y. B. Zhu, L. X. Zheng, J. Y. Ding, Y. Quan, L. M. Wang, B. Qi. *Biosens. Bioelectron.*, 2015, **69**, 174.

[25] H. Zhang, Z. X. Lei, X. Fu, X. C. Deng, Q. Wang, D. Y. Gu. *Sensor. Actuat. B-Chem*., 2017, **246**, 896.

[26] T. Yu, T. T. Zhang, W. Zhao, J. J. Xu, H. Y. Chen. *Talanta*, 2017, **165**, 570.

[27] L. L. Tan, Z. B. Chen, C. Zhang, X. C. Wei, T. H. Lou, Y. Zhao. *Small*, 2017, **13**, 1603370.

[28] X. L. Song, Y. Wang, S. Liu, X. Zhang, H. W. Wang, J. F. Wang, J. D. Huang. *Microchim. Acta*., 2019, **186**, 105.

[29] X. Y. Li, Z. H. Du, S. H. Lin, J. J. Tian, H. T. Tian, W. T. Xu. *Food Chem*., 2020, **316**, 126303.

[30] Z. Xiao, H. Si , L. Deng, L. Long, R. Ju, X. Zhang, Y. Liu. *Biosens. Bioelectron*., 2019, **38**, 840. (in Chinese)

[31] J. Yuan, Y. Wu, X. Kang, H. Liu, Y. Li. *Int. J. Environ. An. Ch.*, 2020, **100**, 841.

[32] A. G. Memon, Y. P. Xing, X. H. Zhou, R. Y. Wang, L. H. Liu, S. Y. Zeng, M. He, M. Ma. *J. Hazard. Mater.*, 2020, **384**, 120948.

[33] F. M. Sang, S. Y. Yin, J. X. Pan, Z. Z. Zhang. *Anal. Bioanal. Chem.*, 2021, **413**, 7001.

[34] A. Ono, H. Togashi. *Ang. Chem. Inter. Ed.*, 2004, **43**, 4300.

[35] K. Chiang, C. Huang, C. Liu, H. Chang. *Anal. Chem*., 2008, **80**, 3716.

[36] H. Wu, X. Liu, J. Jiang, G. Shen, R. Yu. *Chin. J. Chem.*, 2009, **27**, 1543.

[37] X. Zuo, H. Zhang, Q. Zhu, W. Wang, J. Feng. *Biosens. Bioelectron.*, 2016, **85**, 464.

[38] X. Cui, L. Zhu, J. Wu, Y. Hou, P. Wang, Z. Wang, M. Yang. *Biosens. Bioelectron.*, 2015, **63**, 506.

[39] R. Wang, X. Zhou, H. Shi, Y. Luo. *Biosens. Bioelectron*., 2016, **78**, 418.

[40] S. Han, X. Zhou, Y. Tang, M. He, X. Zhang, H. Shi, Y. Xiang. *Biosens. Bioelectron.*, 2016, **80**, 265.

[41] M. Xu, Z. Gao, Q. Wei, G. Chen,D. Tang. *Biosens. Bioelectron.*, 2016, **79**, 411.

[42] W. Yun, W. Xiong, H. Wu, M. Fu, Y. Huang, X. Liu, L. Yang. *Sensor. Actuat. B-Chem.*, 2017, **249**, 493.

[43] Y. Li, N. Liu, H. Liu, Y. Wang, Y. Hao, X. Ma, X. Li, Y. Huo, J. Lu, S. Tang, C. Wang, Y. Zhang, Z. Gao. *Sci. Rep.*, 2017, **7**, 45974.

[44] L. Yu, W. Lan, H. Xu, H. Chen, L. Bai, W. Wang. *Sensor. Actuat. B-Chem.*, 2017, **248**, 411.

[45] A. Ravikuma, P. Panneerselvam. *Analyst*, 2018, **143**, 2623.

[46] X. Zhu, R. Wang, X. Zhou, A. Tan, X. Wen. *Spectros. Spect. Anal.*, 2018, **38**, 3447. (in Chinese)

[47] X. Song, B. Fu, Y. Lan, Y. Chen, Y. Wei, C. Dong. *Spectrochim. Acta A: Mol. Biomol. Spectros.*, 2018, **204**, 301.

[48] H. Xu, F. Geng, X. Jiang, C. Shao, Y. Wang, K. Wang, P. Qu, M. Xu, B. Ye. *Sensor. Actuat. B-Chem.*, 2018, **255**, 1024.

[49] Q. Zhu, L. Liu, Y. Xing, X. Zhou. *J. Hazard. Mater.*, 2018, **355**, 50.

[50] H. Guo,J. Li,Y. Li,D. Wu,H. Ma,Q. Wei,B. Du. *Anal. Chim. Acta*., 2019, **1048**, 161.

[51] Y. Shan, B. Wang, H. Huang, D. Jiang, X. Wu, L. Xue, S. Wang, F. Liu. *Biosens. Bioelectron*., 2019, **132**, 238.

[52] D. Zhou, L. Zeng, J. Pan, Q. Li, J. Chen. *Talanta*, 2020, **207**, 120258.

[53] Z. Li, H. Sun, X. Ma, R. Su, R. Sun, C. Yang, C. Sun. *Anal. Chim. Acta*, 2020, **1099**, 136.

[54] J. Hu, D. Wang, L. Dai, G. Shen, J. Qiu. *Microchem. J*., 2020, **159**, 105562.

[55] J. Y. Wang, C. Y. Du, P. T. Yu, Q. Zhang, H. X. Li, C. Y. Sun. *Sensor. Actuat. B-Chem.*, 2021, **348**, 130707.

[56] X. C. Jin, T. Sun, Z. Y. Wu, D. Y. Wang, F. Hu, J. X. Xu, X. Li, J. Q. Qiu. *Anal. Chim. Acta*., 2022, **1221**, 340113.

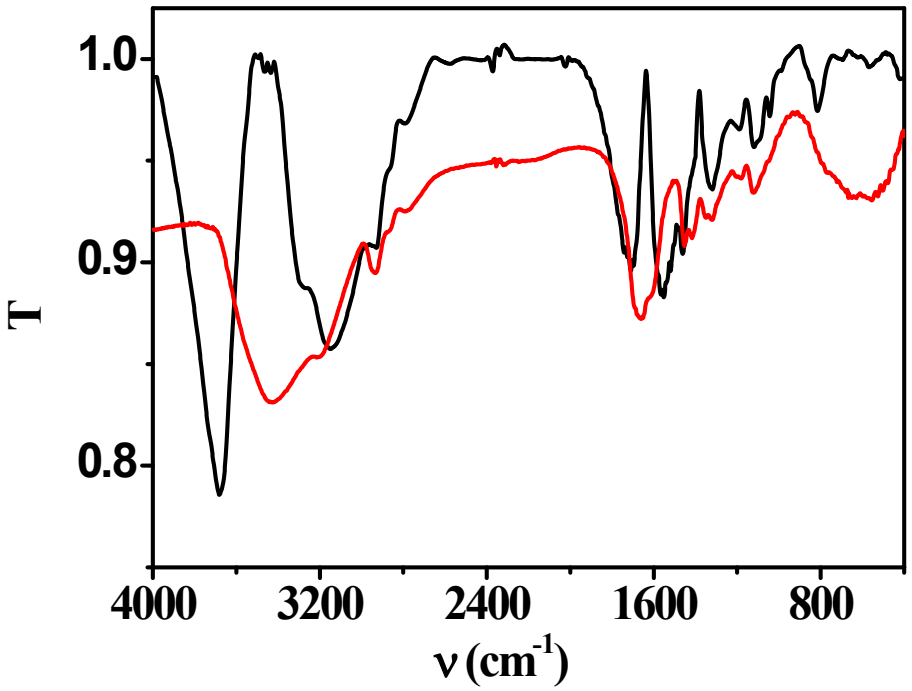

Fig.S11 IR spectra of polyacrylamide and the fluorescent hydrogel

In IR spectra, the red curve is the IR absorption spectrum of polyacrylamide. Peaks 3199.37 cm^{-1} and 3416.61 cm^{-1} representative the symmetric and asymmetric stretching vibration of amide N-H, 1667.40 cm^{-1} stands for the symmetric stretching vibration of C=O, 2936.99 cm^{-1} and 2776.17 cm^{-1} for asymmetric and symmetric stretching vibration of -CH_2-. Peak 1458.62 cm^{-1} belongs to the bending vibration of -CH_2- in the polymer chains; The black curve is the IR absorption spectrum of the obtained fluorescent hydrogel. Compared with polyacrylamide, the most obvious changes take place at the absorption peak of 3416.61 cm^{-1}, 3199.37 cm^{-1}, and 1667.40 cm^{-1}. The position of 3416.61 cm^{-1} and 3199.37 cm^{-1} shifts towards high wave number and gain the strongest absorption peak in 3680.40 cm^{-1}, which should be attributed to the asymmetric stretching vibration of O-H that comes from the

fluorescein monomer; the position of 1667.40 cm^{-1} also shifts towards high wave number and gain a strong absorption peak in 1696.33 cm^{-1} and stands for the symmetric stretching vibration of C=O; meanwhile, a new strong absorption peak appears in 1541.73 cm^{-1}, which should be attributed to the stretching vibration of the C=C from the uracil monomer and the skeleton vibration of the benzene ring from the fluorescein. The above changes in the position of the key absorption peaks indicate that the obtained hydrogel is indeed a uracil and fluorescein functionalized polymer.

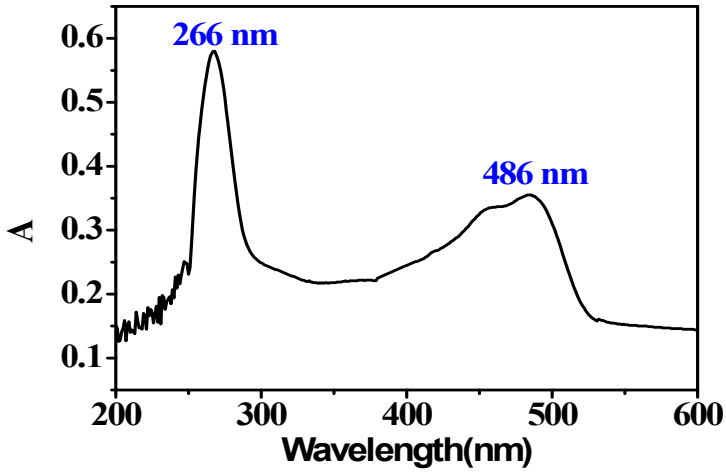

Fig.S12 UV-visible absorption spectra of the fully swollen fluorescent hydrogel